



<sup>8</sup> California Institute of Technology, Pasadena, CA, USA

<sup>9</sup> Jet Propulsion Laboratory, Pasadena, CA, USA

\* now at: NOAA-ESRL, Boulder, CO 80305, USA

Received: 14 March 2011 – Accepted: 26 April 2011 – Published: 12 May 2011

Correspondence to: J. Messerschmidt (messerschmidt@iup.physik.uni-bremen.de)

Published by Copernicus Publications on behalf of the European Geosciences Union.

ACPD

11, 14541–14582, 2011

---

**The IMECC  
campaign: results for  
CO<sub>2</sub>**

J. Messerschmidt et al.

---

Title Page

Abstract

Introduction

Conclusions

References

Tables

Figures

⏪

⏩

◀

▶

Back

Close

Full Screen / Esc

Printer-friendly Version

Interactive Discussion



## Abstract

The Total Carbon Column Observing Network (TCCON) is a ground-based network of Fourier Transform Spectrometer (FTS) sites around the globe, where the column abundances of CO<sub>2</sub>, CH<sub>4</sub>, N<sub>2</sub>O, CO and O<sub>2</sub> are measured. CO<sub>2</sub> is constrained with a precision better than 0.25%. To achieve a similarly high accuracy, calibration to World Meteorological Organization (WMO) standards is required. This paper introduces the first aircraft calibration campaign of five European TCCON sites and a mobile FTS instrument. A series of WMO standards in-situ profiles were obtained over European TCCON sites via aircraft and compared with retrievals of CO<sub>2</sub> column amounts from the TCCON instruments. The results of the campaign show that the FTS measurements are consistently biased 1.0% ± 0.2% low with respect to WMO standards, in agreement with previous TCCON calibration campaigns. The standard a priori profile for the TCCON FTS retrievals is shown to not add a bias. The same calibration factor is generated using aircraft profiles as a priori and with the TCCON standard a priori. With a calibration to WMO standards, the highly precise TCCON CO<sub>2</sub> measurements of total column concentrations provide a suitable database for the calibration and validation of nadir-viewing satellites.

## 1 Introduction

Carbon dioxide (CO<sub>2</sub>) is the most abundant anthropogenic greenhouse gas (GHG), and its increase is driving global climate change. To understand climate change, both the monitoring and the prediction of CO<sub>2</sub> abundances are important. Monitoring is necessary to improve our understanding of processes governing the CO<sub>2</sub> cycle, and it is also of major interest for measuring the success or failure of emission reduction or sequestration. Prediction will become an even more important factor as the consequences of climate change will increasingly affect human and natural systems.

ACPD

11, 14541–14582, 2011

## The IMECC campaign: results for CO<sub>2</sub>

J. Messerschmidt et al.

Title Page

Abstract

Introduction

Conclusions

References

Tables

Figures

⏪

⏩

◀

▶

Back

Close

Full Screen / Esc

Printer-friendly Version

Interactive Discussion



---

**The IMECC  
campaign: results for  
CO<sub>2</sub>**J. Messerschmidt et al.

---

[Title Page](#)[Abstract](#)[Introduction](#)[Conclusions](#)[References](#)[Tables](#)[Figures](#)[◀](#)[▶](#)[◀](#)[▶](#)[Back](#)[Close](#)[Full Screen / Esc](#)[Printer-friendly Version](#)[Interactive Discussion](#)

Currently the sources and sinks of CO<sub>2</sub> are determined by two different approaches: bottom-up and top-down. The former estimates the carbon budget by starting with process information at the scale of a few square meters, requiring upscaling to provide information at regional scales. The latter uses atmospheric inverse transport modeling to derive surface flux distributions from atmospheric concentration measurements. Until recently the top-down approach was solely based on a network of in-situ boundary layer measurement stations. This approach is limited by the sparse spatial coverage of the sampling sites (Marquis and Tans, 2008), but also by the dependence and sensitivity of sink estimates to the assumed vertical model transport (Baker et al., 2006; Stephens et al., 2007).

To improve the constraint on carbon cycle processes and for a global coverage, the space agencies JAXA, ESA, and NASA have launched an ambitious effort to map the integrated column of CO<sub>2</sub> and CH<sub>4</sub> by satellite observations (e.g. GOSAT, CarbonSat, OCO-2). The space-based observations can significantly improve the source-sink estimates by improving the description of the CO<sub>2</sub> distribution, provided they are sufficiently precise and accurate (Rayner and O'Brien, 2001).

TCCON is a worldwide network of ground-based FTSs that was founded in 2004. It has been largely used as a calibration and validation resource for satellite measurements (e.g. Reuter et al., 2011; Morino et al., 2010), but also provides insights into carbon cycle science (e.g. Yang et al., 2007; Keppel-Aleks et al., 2011). The individual TCCON sites are operated by various institutions around the world (e.g. Washenfelder et al., 2006; Wunch et al., 2011; Deutscher et al., 2010; Geibel et al., 2010). TCCON data products are column-averaged dry-air mole fractions, e.g. X<sub>CO<sub>2</sub></sub>, X<sub>CH<sub>4</sub></sub>, X<sub>N<sub>2</sub>O</sub>, X<sub>CO</sub>. TCCON measurements for CO<sub>2</sub> show a precision better than 0.25 % (~1 ppm) (Wunch et al., 2011). Under clear sky conditions, precisions of even 0.1 % can be achieved (Washenfelder et al., 2006; Messerschmidt et al., 2010; Deutscher et al., 2010). With its sufficiently precise measurements of total columns of greenhouse gases, FTIR spectrometry is the most suitable measurement technique to validate and calibrate satellite total column measurements.

To provide the link between satellite measurements and the ground-based in-situ network, a sufficiently accurate constraint of trace gas abundances is of critical importance. Absolute calibration of the TCCON measurements to the WMO calibration scale is achieved using aircraft and balloon profiling above the FTS stations.

5 The first calibration campaign of a TCCON site was described by Washenfelder et al. (2006). The calibration to WMO standards revealed a bias of 2 % for the Park Falls site, and showed an excellent correlation. Deutscher et al. (2010) describe the calibration campaign of the TCCON site in Darwin, Australia and yield a low bias of about 1 % with respect to WMO-standards. Additionally the agreement between Darwin and the first  
10 calibration campaign data was shown. Wunch et al. (2010) included further calibration campaigns of TCCON sites in the United States of America, Japan, and New Zealand and harmonized the calibration method for all sites. All calibration campaigns yield consistently a single calibration factor of  $0.989 \pm 0.002$  for  $\text{CO}_2$ .

This paper introduces the first aircraft calibration campaign of European TCCON  
15 sites with the same TCCON data retrieval as used by Wunch et al. (2010). During the campaign, high altitude in-situ profiles were obtained with an aircraft above five European TCCON sites and a mobile FTS system in Jena, Germany. An overview of the campaign and the results for  $\text{CO}_2$  will be presented in this paper. The results show an European TCCON sites calibration factor for  $\text{CO}_2$  of  $0.989 \pm 0.002$ .

## 20 **2 The IMECC campaign**

The EU project, Infrastructure for Measurement of the European Carbon Cycle (IMECC), is an Integrated Infrastructure Initiative within the Sixth Framework Programme of the European Commission. The aim of the IMECC project is to build the infrastructure necessary for the characterization of the European carbon balance. 30  
25 partners within 15 countries are contributing for four years (2007–2011) in three main initiatives. The first focuses on the improved comparability of European  $\text{CO}_2$  measurements. The second targets on establishing a broad, co-ordinated and accessible

### The IMECC campaign: results for $\text{CO}_2$

J. Messerschmidt et al.

Title Page

Abstract

Introduction

Conclusions

References

Tables

Figures

◀

▶

◀

▶

Back

Close

Full Screen / Esc

Printer-friendly Version

Interactive Discussion



European CO<sub>2</sub> database. The implementation of new measurement approaches is supported in the third initiative.

The first airborne campaign to calibrate FTS sites in Europe with respect to WMO standards (Zhao and Tans, 2006) was funded by the IMECC project. Organization of the flight tracks, the aircraft instrumentation and the post-flight analysis of the aircraft in-situ data was undertaken by the Max Planck Institute for Biogeochemistry (MPI-BGC). The main purpose of the campaign was the calibration of the following European TCCON sites: Bialystok (Poland), Bremen (Germany), Garmisch (Germany), Karlsruhe (Germany), and Orléans (France), and the mobile FTS system located in Jena (Germany), which was built to be deployed at Ascension Island. Figure 1 shows the locations of the calibrated sites and the airbase of the IMECC campaign in Hohn, Germany, are shown.

The calibration flights took place between September 28 and October 9, 2009. The in-situ instrumentation was on board a Learjet 35A, operated by enviscope GmbH (Frankfurt a.M., Germany), with a flight ceiling of 13 km. Near the European TCCON sites, high altitude in-situ profiles were taken, typically from 500 m up to 13 000 m. The lower 5 km were mostly flown in spirals, however, due to e.g. air traffic restrictions, this approach had to be modified at some sites. A typical aircraft profile is shown in Fig. 2.

Additional dips were performed during the transfer flights from the airbase. Overall, eight flights were made on four days. In about 20 flight hours, 16 vertical profiles were generated over the European TCCON sites at solar zenith angles (SZAs) ranging from 51 to 84 degrees. The flight overpasses are listed in Table 1. During all flights, in-situ data were taken for CO<sub>2</sub>, CH<sub>4</sub>, H<sub>2</sub>O, CO, N<sub>2</sub>O, H<sub>2</sub>, SF<sub>6</sub>.

The FTS sites were operated at the time of the campaign by the individual responsible working groups. All European TCCON FTS instruments are Bruker 125HR spectrometers. The settings used during the campaign are listed in Table 2. In the following section, the different sites are described in detail.

## The IMECC campaign: results for CO<sub>2</sub>

J. Messerschmidt et al.

Title Page

Abstract

Introduction

Conclusions

References

Tables

Figures

⏪

⏩

◀

▶

Back

Close

Full Screen / Esc

Printer-friendly Version

Interactive Discussion



## 2.1 Calibrated European TCCON sites

**Bialystok, Poland.** The FTS facility in Bialystok is operated by the Institute of Environmental Physics (IUP), Bremen, Germany in close cooperation with AeroMeteoService, Bialystok, Poland. Bialystok represents the easternmost measurement site within the European Union.

5 An on-site tall tower (300 m) provides boundary layer in-situ measurements. Bialystok and Orléans, France are the only sites with collocated FTS and tall tower measurements in Europe. Additionally, CO<sub>2</sub> profiles up to 2.5 km altitude are measured from small aircraft regularly. The FTS instrument was funded by the EU-projects GEOmon (Global Earth Observation and Monitoring) and IMECC and has been in operation since March 2009. The FTS in Bialystok is fully  
10 automated, and is controlled via remote access (Messerschmidt et al., 2010).

**Bremen, Germany.** FTS measurements were started at the IUP in Bremen in 2000, and the Bremen site has been part of the Network for the Detection of Atmospheric Composition Change (NDACC) and TCCON since 2004. While most European NDACC observatories are  
15 located on high mountains, the Bremen site is located on flat terrain. The low altitude location is advantageous for studying tropospheric gases. In addition, the flat surroundings at the site in Bremen makes this site well suited for the validation of satellites, e.g. (Reuter et al., 2011).

**Garmisch-Partenkirchen, Germany.** The Garmisch FTS site is operated by the Institute for Meteorology and Climate Research Atmospheric Environmental Research (IMK-IFU), which is part of the Karlsruhe Institute of Technology (KIT). Measurements started in 2004 and the site  
20 has been part of TCCON since 2007. This site is located in the alpine region of Southern Germany. The FTS is operated coincident with the NDACC mountain-site FTS at Zugspitze (2964 m a.s.l.). The Garmisch site is close (about 50 km to the south) to the Hohenpeienberg site operated by the German Weather service, where in-situ CO<sub>2</sub> and CH<sub>4</sub> measurements are performed.

25 **Jena, Germany.** The FTS instrument in Jena was set up and operated by the Atmospheric Remote Sensing group at the MPI-BGC. In the long-term, the instrument is destined to be located at Ascension Island in the South Atlantic Ocean. During the time of the IMECC campaign the instrument was still being set up at Jena. After the campaign the FTS system was shipped to Australia, for a comparison campaign with the FTS at the University of Wollongong (Geibel  
30 et al., 2010).

ACPD

11, 14541–14582, 2011

### The IMECC campaign: results for CO<sub>2</sub>

J. Messerschmidt et al.

Title Page

Abstract

Introduction

Conclusions

References

Tables

Figures

◀

▶

◀

▶

Back

Close

Full Screen / Esc

Printer-friendly Version

Interactive Discussion



**Karlsruhe, Germany.** The FTS instrument at the KIT in Karlsruhe has been operational since September 2009, just before the IMECC campaign. It is operated by the Institute for Meteorology and Climate Research – Atmospheric Trace Gases and Remote Sensing (IMK-ASF/KIT).

**Orléans, France.** The automated FTS facility in Orléans is operated by the IUP, Bremen, Germany in close cooperation with the LSCE, Paris, France. The measurement site not far from Orléans has the advantage of an on-site tall-tower (180 m). TCCON measurements started immediately after installation in August 2009. The setup was funded by the IMECC project. The FTS in Orléans is set up in the same manner as the Bialystok instrument.

## 2.2 Aircraft instrumentation

For continuous measurements of CO<sub>2</sub>, CH<sub>4</sub> and H<sub>2</sub>O, the aircraft was equipped with a Wavelength-Scanned Cavity Ring Down Spectrometer (CRDS) (model G1301-m, Picarro Inc., Sunnyvale, CA), providing mixing ratio data recorded at ~0.5 Hz intervals. The analyzer was calibrated against WMO reference gases in the laboratory before and after the airborne campaign, providing an accuracy of 0.1 ppm for CO<sub>2</sub> and 2 ppb for CH<sub>4</sub>. Measurements were made in wet air, and dry-air mixing ratios were derived following the method of Chen et al. (2010). CO data were measured with an Aero-Laser instrument (model AL5002), which was calibrated during flight using WMO traceable standards. The instrument provides dry-air mixing ratios at 1 Hz frequency with an accuracy of 2 ppb (Gerbig et al., 1999). Additionally, up to eight flasks per profile were taken at different altitude levels, from which CO<sub>2</sub>, CH<sub>4</sub>, N<sub>2</sub>O, CO, H<sub>2</sub> and SF<sub>6</sub> were analyzed, validating the quality of the continuous measurements. The flasks were analyzed post-flight at the MPI-BGC's gas analysis lab. Supplemental meteorological data (pressure, temperature, latitude, longitude, altitude, distance to site, and time) were also recorded.

## The IMECC campaign: results for CO<sub>2</sub>

J. Messerschmidt et al.

Title Page

Abstract

Introduction

Conclusions

References

Tables

Figures

⏪

⏩

◀

▶

Back

Close

Full Screen / Esc

Printer-friendly Version

Interactive Discussion



### 3 Data analysis

#### 3.1 European TCCON data

In the FTS instruments JEN, KAR, GAR and BRE the Optics User Software (OPUS version 6.5), a program provided by Bruker, was used to record the interferograms. In BIK and ORL, the raw interferogram data were obtained directly from the embedded web server inside the instruments. To calculate the spectra from the interferograms, we used the Interferogram Processing Package (IPP), which was developed at the Jet Propulsion Laboratory (JPL) (Pasadena, USA) within the framework of TCCON. In the former case, OPUS-IPP (version 20100123) and in the latter case, SLICE-IPP (version 20100123) was used. Both software packages perform the same Fast Fourier Transformation, the different names only indicate the different formats of the interferograms. Additionally, they correct the spectra for solar intensity variations, caused e.g. by passing clouds (Keppel-Aleks et al., 2007). GFIT (version 4.4.10), a nonlinear least-squares spectral fitting algorithm, developed by G. Toon (JPL), was used for the retrieval of the trace gas column amounts from the measured spectra (Wunch et al., 2011). The tropospheric portion of the a priori CO<sub>2</sub> profile, used in GFIT, is based on an empirical model fitting GLOBALVIEW CO<sub>2</sub> data (GLOBALVIEW-CO<sub>2</sub>, 2010). The tropopause height is determined from the National Centers for Environmental Prediction/National Center for Atmospheric Research (NCEP/NCAR) reanalysis. The stratospheric a priori CO<sub>2</sub> decreases with altitude above the tropopause height, depending on the age of the air, based on measurements by Andrews et al. (2001). In order to eliminate a potential bias introduced by the a priori profiles used in the standard TCCON retrieval, the assembled aircraft profiles were used as GFIT a priori (Wunch et al., 2010). The column-averaged dry-air mole fraction (DMF) of the measured gases, e.g. X<sub>CO<sub>2</sub></sub>, can be calculated from the retrieved column amount by

$$X_{\text{CO}_2} = 0.2095 \cdot \frac{1 \text{e}6 \cdot \text{column}_{\text{CO}_2}}{\text{column}_{\text{O}_2}} \quad (1)$$

## The IMECC campaign: results for CO<sub>2</sub>

J. Messerschmidt et al.

[Title Page](#)[Abstract](#)[Introduction](#)[Conclusions](#)[References](#)[Tables](#)[Figures](#)[⏪](#)[⏩](#)[◀](#)[▶](#)[Back](#)[Close](#)[Full Screen / Esc](#)[Printer-friendly Version](#)[Interactive Discussion](#)

---

## The IMECC campaign: results for CO<sub>2</sub>

J. Messerschmidt et al.

---

[Title Page](#)[Abstract](#)[Introduction](#)[Conclusions](#)[References](#)[Tables](#)[Figures](#)[⏪](#)[⏩](#)[◀](#)[▶](#)[Back](#)[Close](#)[Full Screen / Esc](#)[Printer-friendly Version](#)[Interactive Discussion](#)

The units of  $X_{\text{CO}_2}$  are  $\mu\text{mol mol}^{-1}$  and commonly expressed in parts per million [ppm]. Taking the ratio of the atmospheric CO<sub>2</sub> and O<sub>2</sub> columns minimizes systematic and correlated errors present in both retrieved CO<sub>2</sub> and O<sub>2</sub> columns (e.g. pressure errors, influence of the instrumental line shape, Washenfelder et al., 2006; Wunch et al., 2011).

5 The CO<sub>2</sub> column is retrieved for two CO<sub>2</sub> bands centered at 6228 cm<sup>-1</sup> and 6348 cm<sup>-1</sup>, and the RMS-error weighted mean is used to calculate  $X_{\text{CO}_2}$ . Column O<sub>2</sub> is retrieved from the electronic band centered at 7882 cm<sup>-1</sup>. A correction to the air mass dependence, supplied with GFIT and described in Wunch et al. (2011) and Deutscher et al. (2010), was added. Data outside the ranges [0.20–0.22] for O<sub>2</sub>, as well as outside the range [350 ppm–400 ppm] for CO<sub>2</sub> are regarded as outliers in the TCCON standard retrieval and discarded. For the IMECC campaign, the variation of the FTS measurements during the time of the overpasses were used as a filter. Only FTS measurements were considered that had a standard deviation about the mean  $X_{\text{CO}_2}$  less than the standard TCCON precision of 0.25 %. Fewer than 10 % of the data points were removed by this filter.

### 3.2 On-site in-situ measurements at European TCCON sites

At Bremen, Garmisch, and Karlsruhe no on-site in-situ measurements were available. At the other three sites, Bialystok, Jena, and Orléans on-site in-situ facilities are installed and used in the campaign.

20 **Bialystok.** With a height of more than 300 m, the tall tower located at the Bialystok site is one of the tallest in Europe. A variety of atmospheric trace gases have been sampled at five levels (4 m, 23 m, 90 m, 180 m, 300 m) quasi-continuously since 2005. CO<sub>2</sub> volume mixing ratio is measured with a LI-7000 non-dispersive infrared (NDIR) gas analyzer from LI-COR. Further details on additional instruments can be found in Popa et al. (2010).

25 **Jena.** A LI-COR LI-6262 NDIR gas analyzer is mounted on the weather station on the roof of the MPI-BGC in Jena, providing continuous CO<sub>2</sub> measurements, traceable to WMO standards with an accuracy of 0.5 ppm.

**Orléans.** The FTS site near Orléans is located next to the Trainou tall tower observatory, a 180 m tall tower that provides quasi-continuous in-situ measurements of CO<sub>2</sub> and other trace gases from three levels (50 m, 80 m, 180 m). CO<sub>2</sub> is measured with a LI-6252 NDIR gas analyzer from LI-COR.

### 3.3 Aircraft in-situ data

The airborne in-situ data have been merged in the MPI-BGC labs with the flask analysis data using weighting functions corresponding to the flow rate during flask sampling. The averaged concentrations agree within WMO targets for CO<sub>2</sub>, CH<sub>4</sub> and CO with the exception of the two first profiles in Bialystok and the first profile in Orléans. The mean difference is 0.06 ppm for CO<sub>2</sub>. Above 8 km, these flights were affected by a small leak in the pump that provided sample gas to the CRDS, causing the CO<sub>2</sub> and H<sub>2</sub>O measurements to be contaminated by cabin air. CO<sub>2</sub> for those portions of the profiles was taken from the flask data. CH<sub>4</sub> measurements by CRDS showed no significant difference during those periods. For each profile the quality-controlled and corrected data were averaged within pressure intervals of 5 hPa. The uncertainties given for the mixing ratios encompass the uncertainty due to interpolation across missing values (e.g. due to instrument calibration periods), and also include the statistical uncertainty from sampling only a limited number of seconds at each pressure interval. In addition, there is an uncertainty added which is related to the calibration of the standard gases against WMO primary gases (for CO<sub>2</sub> 0.1 ppm, for CH<sub>4</sub> 2 ppb, and for CO 2 ppb). Given the aircraft ceiling of 13 km, the aircraft measurements covered roughly 80 % of the total column in terms of pressure measured from the ground.

### 3.4 Completing the in-situ profiles

In order to compare the FTS data with the high altitude in-situ profiles, the aircraft data have to be extended to the ground and in the stratosphere to cover the CO<sub>2</sub> total column. Therefore the airborne in-situ data are combined with on-site in-situ mea-

## The IMECC campaign: results for CO<sub>2</sub>

J. Messerschmidt et al.

Title Page

Abstract

Introduction

Conclusions

References

Tables

Figures

◀

▶

◀

▶

Back

Close

Full Screen / Esc

Printer-friendly Version

Interactive Discussion



surements, if provided (BIK, ORL, JEN) or extrapolated to the surface with the lowest aircraft measurement (BRE, KAR, GAR). To estimate the stratospheric CO<sub>2</sub> decrease with the age of air (Sect. 3.1), the standard a priori profiles of the FTS retrieval are used for the extension in the stratosphere. The tropopause height is determined from the NCEP reanalysis, supplied in the TCCON standard retrieval. For aircraft profiles that were measured higher than the tropopause, the standard GFIT a priori CO<sub>2</sub> profile was attached to the highest aircraft measurement. For aircraft profiles that were not measured up to the tropopause pressure, the aircraft profile was extended with the most contemporary profile at the site. At the Karlsruhe site, only one overpass was carried out, and the upper troposphere was filled in with the highest aircraft measurement. The GFIT a priori CO<sub>2</sub> profile was then shifted in CO<sub>2</sub> to fit the extended aircraft measurement at the tropopause. All assembled in-situ profiles are shown for each site in Figs. A1–A4. The aircraft measurements are given in red. The GFIT a priori profiles fitted in CO<sub>2</sub> to the aircraft measurements are shown in blue. Extended parts for missing measurements in the upper troposphere are indicated as black and used contemporary profiles in green. The NCEP tropopause height is indicated by a thin red line. The original GFIT a priori profiles are shown with a thin dotted black line. The resulting uncertainties are discussed in Sect. 3.6.

### 3.5 Integration of the assembled in-situ profiles

The completed in-situ profiles over the European TCCON sites can be compared with the FTS DMF, when integrated to compute column-averaged CO<sub>2</sub> DMF. Rodgers and Connor (2003) introduced a method to compare two instruments, of which one has much higher vertical resolution than the other. This approach has been modified by the Wunch et al. (2010) retrieval set up, and is duplicated here.

The averaging kernels are needed for comparison between two instruments. The averaging kernel matrix represents the changes in a retrieved profile at one level  $i$  due to a perturbation to the true profile at another level  $j$ . Since GFIT does a profile scaling retrieval (PSR), the averaging kernel matrix reduces to a vector representing the sensi-

## The IMECC campaign: results for CO<sub>2</sub>

J. Messerschmidt et al.

Title Page

Abstract

Introduction

Conclusions

References

Tables

Figures



Back

Close

Full Screen / Esc

Printer-friendly Version

Interactive Discussion



tivity of the retrieved total column to perturbations of the partial columns at the various atmospheric levels. In GFIT the averaging kernels are calculated with the scaled profiles, therefore the FTS retrieval scaling factor,  $\gamma$ , has to be taken into account (Wunch et al., 2010):

$$\hat{c}_s = \gamma c_a + a^T (x_h - \gamma x_a) \quad (2)$$

with  $\hat{c}_s$ : smoothed DMF of the aircraft,  $\gamma$ : FTS retrieval scaling factor,  $c_a$ : FTS a priori DMF,  $a^T$ : FTS column averaging kernel,  $x_h$ : aircraft profile,  $x_a$ : FTS a priori profile.

The derivation of the equation of the column-averaged aircraft CO<sub>2</sub> DMF can be found in Wunch et al. (2010) and yields:

$$\hat{c}_s = \gamma \frac{VC_{CO_2}^{a\ priori}}{VC_{air}} + \left( \frac{VC_{CO_2,ak}^{aircraft} - \gamma VC_{CO_2,ak}^{a\ priori}}{VC_{air}} \right) \quad (3)$$

with  $\gamma$ : FTS retrieval scaling factor,  $VC_{air}$ : total column of dry-air,  $VC_{CO_2}^{a\ priori}$ : total vertical column of CO<sub>2</sub>,  $VC_{CO_2,ak}^{aircraft}$ : column averaging kernel-weighted vertical column of the aircraft,  $VC_{CO_2,ak}^{a\ priori}$ : column averaging kernel-weighted vertical a priori.

Variability in the averaging kernels is primarily driven by changing solar zenith angles. Therefore the averaging kernel from the FTS measurement nearest in time to the central time of the overpass was used for the smoothing. This averaging kernel is the mean over both CO<sub>2</sub> retrieval windows. The column averaging kernel vectors used for the integration of the 16 in-situ profiles during the IMECC campaign are shown in Fig. 3.

### 3.6 Uncertainty discussion

The Joint Committee for Guides in Metrology (JCGM, 2008) recommendations state that known systematic effects should not simply be encompassed by increasing the

## The IMECC campaign: results for CO<sub>2</sub>

J. Messerschmidt et al.

Title Page

Abstract

Introduction

Conclusions

References

Tables

Figures

◀

▶

◀

▶

Back

Close

Full Screen / Esc

Printer-friendly Version

Interactive Discussion



estimated uncertainty, but rather corrected and the uncertainty in the correction included in the standard uncertainty of the corrected quantity. Therefore, we attempt to treat all known systematic effects in this fashion. The total uncertainty is then calculated as the sum in quadrature of the contributing uncertainty sources for both the FTS measurements and the in-situ profiles.

### 3.6.1 Uncertainty of FTS-derived DMFs

The total uncertainty of the FTS data is determined by two factors: firstly, by the measurement to measurement variability during the overpasses; and secondly by the uncertainty in correcting for a systematic effect introduced by a mis-sampling of the internal reference laser provided in the commercially available FTSs. Messerschmidt et al. (2010) showed that collocated FTS instruments agree within 0.07 %, but only after correcting for this laser sampling problem. Briefly, a periodic laser mis-sampling leads to so called ghosts (artificial spectral lines), which are mirror images of the original spectral lines. The influence of the ghosts on the retrieved  $X_{\text{CO}_2}$  was quantified as a function of the ghost and parent line intensities, called the ghost/parent line ratio (GPR). For a typical GPR, the retrieved  $X_{\text{CO}_2}$  is affected by about 1 ppm. Therefore, a correction scheme was introduced for solar measurements afflicted with ghosts (Messerschmidt et al., 2010). The effect of the retrieved  $X_{\text{CO}_2}$  was quantified and this correction applied to all measurements during the IMECC campaign.

The Messerschmidt et al. (2010) correction scheme does not predict the sign of the ghosts, which means that it is ambiguous as to whether the ghosts lead to an over- or an underestimation of the retrieved  $X_{\text{CO}_2}$ . For three of the FTS instruments (BIK, BRE, ORL), this sign was inferred from the side-by-side measurements detailed by Messerschmidt et al. (2010). For the Garmisch and Karlsruhe FTS instruments, the ghosts were minimized prior to the aircraft campaign and did not introduce a large systematic effect. The Jena instrument could not be corrected prior to the aircraft campaign, and had significant ghosts, which affected the retrievals. The results suggest an over-estimation of  $X_{\text{CO}_2}$ . However, as we cannot be sure of the sign, we investigate two

## The IMECC campaign: results for $\text{CO}_2$

J. Messerschmidt et al.

Title Page

Abstract

Introduction

Conclusions

References

Tables

Figures

◀

▶

◀

▶

Back

Close

Full Screen / Esc

Printer-friendly Version

Interactive Discussion



“worst-case” scenarios in calculation of the scaling factors for the FTS relative to the in-situ profile in Sect. 4. These correspond to all ghosts (Table 3) leading to an (a) under- and (b) over-estimation of the retrieved  $X_{\text{CO}_2}$ . The difference between these scenarios is used to check the correction of the systematic effect introduced by the ghost correction scheme in the calculation of scaling factors.

Due to poor weather situations at Jena and Bremen, not all overpasses could be carried out at the same time as the FTS data were measured (BRE\_1, JEN\_3, JEN\_4). To account for a delay of two hours in all three cases, the expected variation due to the diurnal  $\text{CO}_2$  cycle was accounted for as a systematic effect. At both sites, the magnitude of the diurnal cycle was estimated from the trend of the FTS measurements on the same day. The diurnal cycle was calculated for BRE\_1 by the trend of the FTS data taken for a 2 h time period prior to the overpass and for JEN\_3 and JEN\_4 by the trend of the FTS data measured for a 2.5 h time period after the overpass. The trends were estimated with the FTS data that met the filter criteria introduced in Sect. 3.1 and extrapolated to the overpass time. On-site in-situ measurements showed for the extrapolated time period in Jena a variability of  $\pm 0.5$  ppm and no significant trend that indicate further influence e.g. from local pollution or changing meteorological conditions. For Bremen no on-site in-situ measurements exist. The BRE\_1, JEN\_3, JEN\_4 data are not included in the calculation of the calibration factor, due to the remaining lack of information during the overpasses, but the results will be discussed in Sect. 4.2.

The total uncertainty for the FTS data is the sum in quadrature of the contributing standard uncertainties: the standard deviation about the mean during the overpass, the standard uncertainty of the ghost estimation and the standard uncertainty of the diurnal cycle estimation. Table 3 summarizes the magnitude of the systematic corrections, the uncertainties and the total uncertainty for all overpasses.

### 3.6.2 Uncertainty of the assembled in-situ data

The uncertainty of the assembled in-situ data is derived from the uncertainty of the aircraft measurements, the uncertainties in extrapolating the profiles and the usage of contemporary profiles (Table 4).

## The IMECC campaign: results for $\text{CO}_2$

J. Messerschmidt et al.

Title Page

Abstract

Introduction

Conclusions

References

Tables

Figures



Back

Close

Full Screen / Esc

Printer-friendly Version

Interactive Discussion



---

**The IMECC  
campaign: results for  
CO<sub>2</sub>**J. Messerschmidt et al.

---

[Title Page](#)[Abstract](#)[Introduction](#)[Conclusions](#)[References](#)[Tables](#)[Figures](#)[⏪](#)[⏩](#)[◀](#)[▶](#)[Back](#)[Close](#)[Full Screen / Esc](#)[Printer-friendly Version](#)[Interactive Discussion](#)

The GFIT a priori CO<sub>2</sub> profiles are used to extend the in-situ data above the tropopause, as explained in Sect. 3.4. Thus a typical profile of mean age (Andrews et al., 2001) above the local tropopause is used to calculate the lag of stratospheric CO<sub>2</sub> values with respect to mean tropospheric values. Furthermore a decrease of the seasonal cycle with altitude is taken into account. Seasonally resolved aircraft measurements during the SPURT project (Engel et al., 2006) revealed that the seasonal cycle in the lowermost stratosphere (i.e. the region of the stratosphere between the local tropopause and the 380 K isentrope) is not only attenuated with increasing vertical distance to the local tropopause but is also shifted with respect to the troposphere (Hoor et al., 2004; Bönisch et al., 2008, 2009; Hintsa et al., 1998). The seasonal cycle magnitude can be as large as 3 ppm at the mid latitude tropopause and decreases to about half of that value at about 50 K potential temperature above the local tropopause. The amplitude and timing of the seasonal cycle at the tropopause is captured quite well in the a priori profiles with a maximum in May. The variability in this area is, however, very high, especially when using pressure coordinates. Therefore a conservative uncertainty estimate is used by assuming that the CO<sub>2</sub> seasonal cycle in the lowermost stratosphere can not be correctly represented and that this seasonal cycle leads to an additional uncertainty of the CO<sub>2</sub> a priori profile of about 2 ppm, that is a typical amplitude of the seasonal cycle in the lowermost stratosphere. This uncertainty is independent of contributions from the absolute uncertainty of the mean age profile, that is estimated to be about 0.3 ppm (Wunch et al., 2010). The total uncertainty of the stratospheric CO<sub>2</sub> values is thus estimated as the sum in quadrature and on the order of 2.02 ppm.

For some overpasses, the profiles could not be measured up to the tropopause. If no contemporary aircraft profile was available, the upper troposphere was filled with the highest aircraft measurement; e.g. as clearly seen in Fig. A2. The CO<sub>2</sub> variability in the upper troposphere, measured at the European TCCON sites, is within 2 ppm and applied as uncertainty for the filling. If a contemporary aircraft profile was available, it was used to estimate the profile above the last aircraft measurement (Figs. A1, A3,

A4). It is assumed that the profile can therewith be better estimated than by using the highest aircraft measurement and an uncertainty of 1.5 ppm is assigned.

For the aircraft data, the standard uncertainty provided by the post-flight analysis at the MPI-BGC's lab was applied. The uncertainties given for the mixing ratios contain uncertainties from extension with the lowest aircraft measurement to the surface pressure, as well as from interpolation across missing values (e.g. due to instrument calibration periods). Also included is the statistical uncertainty from sampling only a limited number of seconds at each pressure interval. In addition, an uncertainty related to the calibration of the standard gases (working tanks) against WMO primary gases is added. The mean standard deviation for the IMECC campaign aircraft profiles is 0.11 ppm. The total uncertainty is calculated from the sum in quadrature of these contributing uncertainties weighted by their relative contribution to the completed profile in terms of pressure.

Due to poor weather conditions a profile was not flown above the Karlsruhe TCCON site. Aircraft measurements were, however, recorded during a stop-over 50 km to the south of the site. The Karlsruhe data are therefore treated similarly to the other overflights, but because of these exceptional circumstances, they are not included in the calculation of the calibration factor. They will be discussed in Sect. 4.2.

The resulting uncertainties for the FTS measurements and for the integrated column-averaged assembled aircraft CO<sub>2</sub> profiles are listed for all overpasses in Table 5.

## 4 Comparison of the European TCCON CO<sub>2</sub> measurements with in-situ data

### 4.1 Comparison to previous TCCON calibrations

The IMECC results can be compared with previous TCCON calibrations, published in Wunch et al. (2010), by predicting a linear relationship and no intercept. The results are plotted in addition to the previous TCCON calibrations presented in Wunch et al. (2010) in Fig. 4. The IMECC data are shown in red and the previous TCCON calibrations in

## The IMECC campaign: results for CO<sub>2</sub>

J. Messerschmidt et al.

Title Page

Abstract

Introduction

Conclusions

References

Tables

Figures

◀

▶

◀

▶

Back

Close

Full Screen / Esc

Printer-friendly Version

Interactive Discussion



green. The best fit to the IMECC data is calculated by considering both errors on the x- and y-axis (York et al., 2004) and is indicated with a red line. The previous TCCON calibrations are shown with a green line. The thin blue lines show the best fits under the worst-case ghost scenarios. The resulting scale factors are reported as the slope of the best fit  $\pm$ two standard deviations. The scale factor, the best fit uncertainty and the scale factor uncertainty are listed in comparison to the previous TCCON calibrations in Table 6.

The worst-case ghost scenarios yield scale factors that lie within the uncertainty of the IMECC calibration scale factor, which implies a correct elimination of the systematic effect by the ghost correction scheme. The larger difference for the upper bound (maximum overestimation) is mostly due to the large ghosts found in the Jena instrument ( $X_{\text{CO}_2} + 1.63$  ppm).

The IMECC calibration scale factor calculated here to be  $0.989 \pm 0.002$  agrees with the Wunch et al. (2010) calibration ( $0.989 \pm 0.002$ ). The IMECC calibration confirms the assumption of one global scale factor for  $\text{CO}_2$  for all TCCON sites worldwide (Wunch et al., 2010), which can be applied independent of site and season. However, the previous TCCON calibrations did not include a correction of potential ghosts in the FTS spectra.

## 4.2 Calibration of the TCCON standard $X_{\text{CO}_2}$ product

FTS data collected during the IMECC campaign were also fitted using the standard GFIT a priori profiles in order to analyze the standard TCCON retrieval. This approach allows estimation of the quality of TCCON  $\text{CO}_2$  data products obtained using the standard GFIT a priori profiles. The mean of all results for the FTS data and the integrated in-situ profiles are listed in comparison with the former retrieval approach in Table 7. The differences in the  $X_{\text{CO}_2}$  are calculated as the FTS retrieval with TCCON standard a priori minus the FTS retrieval with the aircraft a priori. The estimation of the scale factor was performed following Sect. 4.1. A linear relationship and a zero intercept was predicted, the best fit was estimated with the York et al. (2004) fitting method, and

### The IMECC campaign: results for $\text{CO}_2$

J. Messerschmidt et al.

Title Page

Abstract

Introduction

Conclusions

References

Tables

Figures

⏪

⏩

◀

▶

Back

Close

Full Screen / Esc

Printer-friendly Version

Interactive Discussion



the KAR\_1, BRE\_1, JEN\_3, and JEN\_4 data are excluded in the fitting procedure. The IMECC data, retrieved with the standard GFIT a priori, are shown in Fig. 5 as filled circles (Bialystok: red, Bremen: purple, Garmisch: cyan, Jena: green, Karlsruhe: yellow, Orléans: blue). The unconsidered KAR\_1, BRE\_1, JEN\_3, and JEN\_4 data are shown in the site corresponding color with red circles. The corresponding retrievals, with the aircraft profiles as a priori, are given as circles in the same color. The scale factor is consistent with the results of Sect. 4.1. All scale factors are listed in Table 8.

The KAR\_1, BRE\_1, JEN\_3, and JEN\_4 data were excluded because of missing information about the exact atmospheric profile during the FTS measurements. In the case of KAR\_1 data, the recorded aircraft profile was displaced, and in the case of the BRE\_1, JEN\_3, and JEN\_4 data the aircraft profiles were not contemporary with the FTS measurements. The latter profiles were corrected for a systematic effect of a diurnal cycle of the order of the FTS measurement precision magnitude (Table 3). The scale factor, calculated including the KAR\_1, BRE\_1, JEN\_3, and JEN\_4 data, yields within their uncertainty the same scale factor as without the data. The Karlsruhe data, however, exhibit an overestimation with respect to the best fit, that can not be investigated due to the lack of information. Model simulations could help to assess potential influence from pollution by nearby emissions at the Karlsruhe site.

We also performed retrievals using an a priori profile based on the true profile shape by taking into account dilution by water vapor, which also yields correction factors that agree within their uncertainties. GFIT retrievals use an a priori profile that is based on dry-air mole fractions. In reality, the FTS observes a profile shape with respect to pressure that is described by the wet-air mole fractions. We investigated the effect of this assumption by comparing retrievals with the aircraft dry-air profile as a priori with retrievals made by creating an a priori wet-air profile by using the co-measured H<sub>2</sub>O profile. The FTS-retrieved  $X_{\text{CO}_2}$  values on average differ by  $0.1 \mu\text{mol mol}^{-1}$ , with the wet-air profile yielding higher columns. However, the application of the averaging kernel and a priori dependent smoothing to the in-situ profile means that these are similarly affected, and individual ratios of aircraft/FTS  $X_{\text{CO}_2}$  do not change. The FTS

## The IMECC campaign: results for CO<sub>2</sub>

J. Messerschmidt et al.

[Title Page](#)[Abstract](#)[Introduction](#)[Conclusions](#)[References](#)[Tables](#)[Figures](#)[⏪](#)[⏩](#)[◀](#)[▶](#)[Back](#)[Close](#)[Full Screen / Esc](#)[Printer-friendly Version](#)[Interactive Discussion](#)

retrieval is therefore insensitive to the a priori profile shape in comparison studies with other measurements (or models). This confirms that the a priori profiles used in GFIT do not add any systematic biases to the results of comparisons between FTS  $X_{\text{CO}_2}$  and other measurements.

## 5 Summary and outlook

The IMECC campaign show a negative bias of  $1\% \pm 0.2\%$  of the FTS  $X_{\text{CO}_2}$  measurements with respect to WMO standards. The negative bias is likely due to spectroscopic inaccuracies, as the aircraft profiles were used as a priori profiles. The results from the IMECC campaign are in very good agreement with previous TCCON calibrations and the findings confirm the TCCON calibration published in Wunch et al. (2010) for five new European TCCON sites.

The IMECC campaign was retrieved with the standard GFIT  $\text{CO}_2$  a priori. The standard GFIT  $\text{CO}_2$  a priori does not add a bias and the results agree with the results obtained with the aircraft profiles as a priori. The findings show that the TCCON standard  $X_{\text{CO}_2}$  product can be measured by instruments using the standard GFIT a priori profiles with a bias of  $1\% \pm 0.2\%$  with respect to WMO standards and a precision of  $0.25\%$ . With calibrated, high precision FTS measurements, TCCON provides an ideal resource for the calibration and validation of satellite measurements as it measures the same quantity as satellites but with a higher precision and accuracy. The European TCCON standard  $X_{\text{CO}_2}$  product accuracy could be estimated to be  $0.8\text{ ppm}$ .

The calibration could firstly be improved by minimizing potential ghosts prior to a calibration campaign and a reliable ghost sign determination in the analysis. Secondly the uncertainty in the in-situ profile is dominated by the sections of the atmosphere not measured by the aircraft. With a jet aircraft flying at maximum flight altitude, roughly  $80\%$  of the total column in terms of pressure can be sampled. The very accurate in-situ measurements have to be extrapolated in the stratosphere, that contribute to a large part of the uncertainty. This should be improved by extending the in-situ measurements

## The IMECC campaign: results for $\text{CO}_2$

J. Messerschmidt et al.

Title Page

Abstract

Introduction

Conclusions

References

Tables

Figures

◀

▶

◀

▶

Back

Close

Full Screen / Esc

Printer-friendly Version

Interactive Discussion



to higher altitudes, for example with balloon or AirCore measurements (Karion et al., 2010) for a further accurate constraint of the calibration factor.

*Acknowledgements.* We acknowledge the support of the European Commission within the 6<sup>th</sup> Framework Program through the Integrated Infrastructure Initiative IMECC (Infrastructure for Measurement of the European Carbon Cycle) and the Integrated Project GEOmon (Global Earth Observation and Monitoring).

The aircraft measurements would not have been possible without the great support from Enviscope GmbH (Frankfurt am Main, Germany), especially Rolf Maser and Christoph Klaus, who were responsible for the aircraft instrument integration and operation. We would also like to thank the Gesellschaft für Flugziieldarstellung mbH (Hohn, Germany), especially Svend Engemann and the other pilots, for their excellent support with flight planning and flight operations. We thank the Polish Air Navigation Services Agency for the organization of the overpass in Bialystok, Poland.

At the Institute of Environmental Physics (Bremen, Germany) Katinka Petersen, Christof Petri, Benjamin Sampson and Christine Weinzierl have contributed greatly to the success of the campaign. From the Max Planck Institute for Biogeochemistry (Jena, Germany) we would like to thank Stephan Baum, Armin Jordan, Martin Hertel, Karl Kübler, and Bert Steinberg for their contributions. We thank the members of RAMCES team at LSCE (Gif-sur-Yvette, France) for maintaining the Orléans FTS site and providing station logistics. We would also like to thank Peter Rayner at the University of Melbourne, Australia for the coordination of the project IMECC and helpful comments on the article.

Implementation of TCCON data processing is supported by a grant from NASA's Carbon Cycle Program (NNX08AI86G) to the California Institute of Technology. Part of this work was performed at the Jet Propulsion Laboratory, California Institute of Technology, under contract with NASA.

## The IMECC campaign: results for CO<sub>2</sub>

J. Messerschmidt et al.

Title Page

Abstract

Introduction

Conclusions

References

Tables

Figures



Back

Close

Full Screen / Esc

Printer-friendly Version

Interactive Discussion



## References

- Andrews, A. E., Boering, K. A., Daube, B. C., Wofsy, S. C., Loewenstein, M., Jost, H., Podolske, J. R., Webster, C. R., Herman, R. L., Scott, D. C., Flesch, G. J., Moyer, E. J., Elkins, J. W., Dutton, G. S., Hurst, D. F., Moore, F. L., Ray, E. A., Romashkin, P. A., and Strahan, S. E.: Mean ages of stratospheric air derived from in situ observations of CO<sub>2</sub>, CH<sub>4</sub>, and N<sub>2</sub>O, J. Geophys. Res., 106, 32295–32314, 2001. 14549, 14556
- Baker, D. F., Law, R. M., Gurney, K. R., Rayner, P., Peylin, P., Denning, A. S., Bousquet, P., Bruhwiler, L., Chen, Y.-H., Ciais, P., Fung, I. Y., Heimann, M., John, J., Maki, T., Maksyutov, S., Masarie, K., Prather, M., Pak, B., Taguchi, S., and Zhu, Z.: TransCom 3 inversion intercomparison: Impact of transport model errors on the interannual variability of regional CO<sub>2</sub> fluxes, 1988–2003, Global Biogeochem. Cy., 20, GB1002, <http://dx.doi.org/10.1029/2004GB002439>, 2006. 14544
- Bönisch, H., Hoor, P., Gurk, Ch., Feng, W., Chipperfield, M., Engel, A., and Bregman, B.: Model evaluation of CO<sub>2</sub> and SF<sub>6</sub> in the extratropical UT/LS region, J. Geophys. Res., 113, D06101, doi:10.1029/2007JD008829, 2008. 14556
- Bönisch, H., Engel, A., Curtius, J., Birner, Th., and Hoor, P.: Quantifying transport into the lowermost stratosphere using simultaneous in-situ measurements of SF<sub>6</sub> and CO<sub>2</sub>, Atmos. Chem. Phys., 9, 5905–5919, doi:10.5194/acp-9-5905-2009, 2009. 14556
- Chen, H., Winderlich, J., Gerbig, C., Hofer, A., Rella, C. W., Crosson, E. R., Van Pelt, A. D., Steinbach, J., Kolle, O., Beck, V., Daube, B. C., Gottlieb, E. W., Chow, V. Y., Santoni, G. W., and Wofsy, S. C.: High-accuracy continuous airborne measurements of greenhouse gases (CO<sub>2</sub> and CH<sub>4</sub>) using the cavity ring-down spectroscopy (CRDS) technique, Atmos. Meas. Tech., 3, 375–386, doi:10.5194/amt-3-375-2010, 2010. 14548
- Deutscher, N. M., Griffith, D. W. T., Bryant, G. W., Wennberg, P. O., Toon, G. C., Washenfelder, R. A., Keppel-Aleks, G., Wunch, D., Yavin, Y., Allen, N. T., Blavier, J.-F., Jiménez, R., Daube, B. C., Bright, A. V., Matross, D. M., Wofsy, S. C., and Park, S.: Total column CO<sub>2</sub> measurements at Darwin, Australia – site description and calibration against in situ aircraft profiles, Atmos. Meas. Tech. Discuss., 3, 989–1021, doi:10.5194/amtd-3-989-2010, 2010. 14544, 14545, 14550
- Engel, A., Bönisch, H., Brunner, D., Fischer, H., Franke, H., Günther, G., Gurk, C., Hegglin, M., Hoor, P., Königstedt, R., Krebsbach, M., Maser, R., Parchatka, U., Peter, T., Schell, D., Schiller, C., Schmidt, U., Spelten, N., Szabo, T., Weers, U., Wernli, H., Wetter, T., and

## The IMECC campaign: results for CO<sub>2</sub>

J. Messerschmidt et al.

Title Page

Abstract

Introduction

Conclusions

References

Tables

Figures

◀

▶

◀

▶

Back

Close

Full Screen / Esc

Printer-friendly Version

Interactive Discussion



Wirth, V.: Highly resolved observations of trace gases in the lowermost stratosphere and upper troposphere from the Spurt project: an overview, *Atmos. Chem. Phys.*, 6, 283–301, doi:10.5194/acp-6-283-2006, 2006. 14556

5 Geibel, M. C., Gerbig, C., and Feist, D. G.: A new fully automated FTIR system for total column measurements of greenhouse gases, *Atmos. Meas. Tech.*, 3, 1363–1375, doi:10.5194/amt-3-1363-2010, 2010. 14544, 14547

Gerbig, C., Schmitgen, S., Kley, D., Volz-Thomas, A., Dewey, K., and Haaks, D.: An improved fast-response vacuum-UV resonance fluorescence CO instrument, *J. Geophys. Res.*, 104, 1699–1704, 1999. 14548

10 GLOBALVIEW-CO2: Cooperative Atmospheric Data Integration Project – Carbon Dioxide, NOAA-ESRL, Boulder, Colorado, cD-ROM, 2010. 14549

Hints, E. J., Boering, K. A., Weinstock, E. M., Anderson, J. G., Gary, B. L., Pfister, L., Daube, B. C., Wofsy, S. C., Loewenstein, M., Podolske, J. R., Margitan, J. J., and Bui, T. P.: Troposphere-stratosphere transport in the lowermost stratosphere from measurements of H<sub>2</sub>O, CO<sub>2</sub>, N<sub>2</sub>O and O<sub>3</sub>, *Geophys. Res. Lett.*, 25, 2655–2658, doi:10.1029/98GL01797, 1998. 14556

Hoor, P., Gurk, C., Brunner, D., Hegglin, M. I., Wernli, H., and Fischer, H.: Seasonality and extent of extratropical TST derived from in-situ CO measurements during SPURT, *Atmos. Chem. Phys.*, 4, 1427–1442, doi:10.5194/acp-4-1427-2004, 2004. 14556

20 JCGM: Evaluation of measurement data – Guide to the expression of uncertainty in measurement, Tech. rep., Joint Committee for Guides in Metrology, Working Group 1, 2008. 14553

Karion, A., Sweeney, C., Tans, P., and Newberger, T.: AirCore: An Innovative Atmospheric Sampling System, *J. Atmos. Ocean. Technol.*, 27, 1839–1853, doi:10.1175/2010JTECHA1448.1, 2010. 14561

25 Keppel-Aleks, G., Toon, G. C., Wennberg, P. O., and Deutscher, N. M.: Reducing the impact of source brightness fluctuations on spectra obtained by Fourier-transform spectrometry, *Appl. Optics*, 46, 4774–4779, 2007. 14549

Keppel-Aleks, G., Wennberg, P. O., and Schneider, T.: Sources of variations in total column carbon dioxide, *Atmos. Chem. Phys.*, 11, 3581–3593, doi:10.5194/acp-11-3581-2011, 2011. 14544

30 Marquis, M. and Tans, P.: Carbon Crucible, *Science*, 320, 460–461, 2008. 14544

Messerschmidt, J., Macatangay, R., Notholt, J., Petri, C., Warneke, T., and Weinzierl, C.: Side by side measurements of CO<sub>2</sub> by ground-based Fourier transform spectrometry (FTS), *Tellus*

- B, 62, 749–758, doi:10.1111/j.1600-0889.2010.00491.x, 2010. 14544, 14547, 14554, 14568  
Morino, I., Uchino, O., Inoue, M., Yoshida, Y., Yokota, T., Wennberg, P. O., Toon, G. C., Wunch,  
D., Roehl, C. M., Notholt, J., Warneke, T., Messerschmidt, J., Griffith, D. W. T., Deutscher,  
N. M., Sherlock, V., Connor, B., Robinson, J., Sussmann, R., and Rettinger, M.: Preliminary  
5 validation of column-averaged volume mixing ratios of carbon dioxide and methane retrieved  
from GOSAT short-wavelength infrared spectra, *Atmos. Meas. Tech. Discuss.*, 3, 5613–5643,  
doi:10.5194/amtd-3-5613-2010, 2010. 14544
- Popa, M. E., Gloor, M., Manning, A. C., Jordan, A., Schultz, U., Haensel, F., Seifert, T.,  
and Heimann, M.: Measurements of greenhouse gases and related tracers at Bialystok  
10 tall tower station in Poland, *Atmos. Meas. Tech.*, 3, 407–427, doi:10.5194/amt-3-407-2010,  
2010. 14550
- Rayner, P. J. and O'Brien, D. M.: The utility of remotely sensed CO<sub>2</sub> concentration data in  
surface source inversions, *Geophys. Res. Lett.*, 28, 175–178, doi:10.1029/2000GL011912,  
2001. 14544
- 15 Reuter, M., Bovensmann, H., Buchwitz, M., Burrows, J. P., Connor, B., Deutscher, N. M., Grif-  
fith, D. W. T., Heymann, J., Keppel-Aleks, G., Messerschmidt, J., Notholt, J., Petri, C., Robin-  
son, J., Schneising, O., Sherlock, V., Velasco, V. A., Warneke, T., Wennberg, P. O., and  
Wunch, D.: Retrieval of atmospheric CO<sub>2</sub> with enhanced accuracy and precision from Scia-  
machy: Validation with Fourier transform spectrometer measurements and comparison with  
20 model results, *J. Geophys. Res.*, 116, D04301, doi:10.1029/2010JD015047, 2011. 14544,  
14547
- Rodgers, C. D. and Connor, B. J.: Intercomparison of remote sounding instruments, *J. Geo-  
phys. Res.*, 108, 4116, doi:10.1029/2002JD002299, 2003. 14552
- Stephens, B. B., Gurney, K. R., Tans, P. P., Sweeney, C., Peters, W., Bruhwiler, L., Ciais,  
25 Philippe AN DRamonet, M., Bousquet, P., Nakazawa, T., Aoki, S., Machida, T., Inoue,  
G., Vinnichenko, N., Lloyd, J., Jordan, A., Heimann, M., Shibistova, O., Langenfelds, Ray  
L. ANDSteele, L. P., Francey, R. J., and Denning, A. S.: Weak Northern and Strong Tropical  
Land Carbon Uptake from Vertical Profiles of Atmospheric CO<sub>2</sub>, *Science*, 316, 1732–1735,  
doi:10.1126/science.1137004, 2007. 14544
- 30 Washenfelder, R., Toon, G., Blavier, J.-F., Yang, Z., Allen, N., Wennberg, P., Vay, S., Matross,  
D., and Daube, B.: Carbon dioxide column abundances at the Wisconsin Tall Tower site, *J.  
Geophys. Res.*, 111, 1–11, doi:10.1029/2006JD007154, 2006. 14544, 14545, 14550
- Wunch, D., Toon, G. C., Wennberg, P. O., Wofsy, S. C., Stephens, B. B., Fischer, M. L., Uchino,

---

## The IMECC campaign: results for CO<sub>2</sub>

J. Messerschmidt et al.

---

Title Page

Abstract

Introduction

Conclusions

References

Tables

Figures

◀

▶

◀

▶

Back

Close

Full Screen / Esc

Printer-friendly Version

Interactive Discussion



## The IMECC campaign: results for CO<sub>2</sub>

J. Messerschmidt et al.

Title Page

Abstract

Introduction

Conclusions

References

Tables

Figures

◀

▶

◀

▶

Back

Close

Full Screen / Esc

Printer-friendly Version

Interactive Discussion



O., Abshire, J. B., Bernath, P., Biraud, S. C., Blavier, J.-F. L., Boone, C., Bowman, K. P., Browell, E. V., Campos, T., Connor, B. J., Daube, B. C., Deutscher, N. M., Diao, M., Elkins, J. W., Gerbig, C., Gottlieb, E., Griffith, D. W. T., Hurst, D. F., Jiménez, R., Keppel-Aleks, G., Kort, E. A., Macatangay, R., Machida, T., Matsueda, H., Moore, F., Morino, I., Park, S., Robinson, J., Roehl, C. M., Sawa, Y., Sherlock, V., Sweeney, C., Tanaka, T., and Zondlo, M. A.: Calibration of the Total Carbon Column Observing Network using aircraft profile data, *Atmos. Meas. Tech.*, 3, 1351–1362, doi:10.5194/amt-3-1351-2010, 2010. 14545, 14549, 14552, 14553, 14556, 14557, 14558, 14560, 14571, 14577

Wunch, D., Toon, G. C., Blavier, J.-F. L., Washenfelder, R., Notholt, J., Connor, B. J., Griffith, D. W. T., Sherlock, V., and Wennberg, P. O.: The Total Carbon Column Observing Network (TC-CON), will be published soon, 369, 2087–2112, doi:10.1098/rsta.2010.0240 2011. 14544, 14549, 14550

Yang, Z., Washenfelder, R., Keppel-Aleks, G., Krakauer, N., Randerson, J., Tans, P., Sweeney, C., and Wennberg, P.: New constraints on Northern Hemisphere growing season net flux, *Geophys. Res. Lett.*, 34, L12807, doi:10.1029/2007GL029742, 2007. 14544

York, D., Evensen, N. M., Martinez, M. L., and De Basabe Delgado, J.: Unified equations for the slope, intercept, and standard errors of the best straight line, *American Journal of Physics*, 72(3), 367, doi:10.1119/1.1632486, 2004. 14558

Zhao, C. L. and Tans, P. P.: Estimating uncertainty of the WMO mole fraction scale for carbon dioxide in air, *J. Geophys. Res.*, 111, D08S09, doi:10.1029/2005JD006003, 2006. 14546

**Table 1.** Site locations and overpass times and codes.

Site	Lat. [° N]	Long. [° E]	Alt. [m a.s.l.]	Overpass: Date/Time [UTC]	Code
Bialystok, Poland	53.23	23.03	180	30 Sep 09:39 10:04 13:48 14:10	BIK_1 BIK_2 BIK_3 BIK_4
Orléans, France	47.97	2.13	132	2 Oct 06:36 07:02 10:35 10:57	ORL_1 ORL_2 ORL_3 ORL_4
Karlsruhe, Germany	49.08	8.43	115	2 Oct 09:31	KAR_1
Garmisch- Parten- kirchen, Germany	47.48	11.06	743	5 Oct 08:47	GAR_1
Jena, Germany	50.91	11.57	211	5 Oct 07:56 08:08 9 Oct 10:12 10:35	JEN_1 JEN_2 JEN_3 JEN_4
Bremen, Germany	53.10	8.85	5	5 Oct 11:29 9 Oct 6 10:52	BRE_1 BRE_2

## The IMECC campaign: results for CO<sub>2</sub>

J. Messerschmidt et al.

Title Page

Abstract

Introduction

Conclusions

References

Tables

Figures

◀

▶

◀

▶

Back

Close

Full Screen / Esc

Printer-friendly Version

Interactive Discussion



## The IMECC campaign: results for CO<sub>2</sub>

J. Messerschmidt et al.

Title Page

Abstract

Introduction

Conclusions

References

Tables

Figures

◀

▶

◀

▶

Back

Close

Full Screen / Esc

Printer-friendly Version

Interactive Discussion



**Table 2.** Instrument settings for the FTS measurements during the IMECC campaign. With <sup>a</sup> resolution =  $\frac{0.9}{\text{OPD}_{\text{max}}}$ , <sup>b</sup> reduced beam diameter for InGaAs via additional aperture, <sup>c</sup> intensity attenuator at the InGaAs diode, <sup>d</sup> due to technical difficulties only forward scans were recorded on the first overflight day, <sup>e</sup> electronic and optical filter are used to prevent Aliasing.

Parameter	JEN	BRE, BIK ORL	GAR	KAR
resolution <sup>a</sup> [cm <sup>-1</sup> ]	0.014	0.014	0.02	0.014
aperture [mm]	1.0 <sup>b</sup>	1.0 <sup>c</sup>	1.0 <sup>c</sup>	0.8
scanner vel. [kHz]	10	10	7.5	20
high pass filter <sup>e</sup>	open	open	open	open
low pass filter <sup>e</sup> [cm <sup>-1</sup> ]	15 798	15 798	15 798	15 798
optical filter <sup>e</sup>	none	dichroic	dichroic	none
scans [no]	1 <sup>d</sup> (FW/BW)	1 (FW/BW)	1 (FW/BW)	6–8
HCL cell	yes	yes	yes	no

**Table 3.** Systematic effects due to ghosts and a time delay between the overpass and FTS measurements and the uncertainty sources contributing to the total uncertainty of the FTS measurements. The total uncertainty accounts for the FTS measurements variability during the overpasses, an uncertainty in the estimation of the expected variation due to the diurnal cycle and the uncertainty in the ghost estimation, according to Messerschmidt et al. (2010).

code	systematic effects [ppm] correction of		uncertainties [ppm]			total
	ghosts with	time delay with	ghosts	time delay	overpass variability	
BIK_1	-0.27	-	0.05	-	0.12	0.13
BIK_2	-0.27	-	0.05	-	0.13	0.14
BIK_3	-0.27	-	0.05	-	0.19	0.20
BIK_4	-0.27	-	0.05	-	0.19	0.20
BRE_1	+0.31	+0.07	0.06	0.01	0.41	0.41
BRE_2	+0.31	-	0.06	-	0.38	0.39
GAR_1	+0.06	-	0.02	-	0.35	0.35
JEN_1	-1.63	-	0.16	-	0.35	0.39
JEN_2	-1.63	-	0.16	-	0.35	0.39
JEN_3	-1.63	+0.37	0.16	0.03	0.26	0.31
JEN_4	-1.63	+0.30	0.16	0.03	0.26	0.31
KAR_1	-0.12	-	0.04	-	0.35	0.35
ORL_1	+0.38	-	0.08	-	0.33	0.34
ORL_2	+0.38	-	0.08	-	0.34	0.35
ORL_3	+0.38	-	0.08	-	0.40	0.41
ORL_4	+0.38	-	0.08	-	0.38	0.39

**The IMECC  
campaign: results for  
CO<sub>2</sub>**

J. Messerschmidt et al.

Title Page

Abstract Introduction

Conclusions References

Tables Figures

◀ ▶

◀ ▶

Back Close

Full Screen / Esc

Printer-friendly Version

Interactive Discussion



## The IMECC campaign: results for CO<sub>2</sub>

J. Messerschmidt et al.

Title Page

Abstract

Introduction

Conclusions

References

Tables

Figures

◀

▶

◀

▶

Back

Close

Full Screen / Esc

Printer-friendly Version

Interactive Discussion



**Table 4.** Contributing uncertainties to the total uncertainty of the assembled in-situ data. The total uncertainty is calculated by the sum in quadrature of the weighted fraction in terms of pressure with respect to the completed in-situ profile.

Uncertainties contributing to the total uncertainty	[ppm]
stratospheric extrapolation	2.02
missing tropospheric values	2.00
usage of contemporary profile	1.50
mean aircraft profile	0.11

## The IMECC campaign: results for CO<sub>2</sub>

J. Messerschmidt et al.

**Table 5.** The IMECC campaign results: the code of each overpass, the type, the solar zenith angle (SZA), the aircraft ceiling/floor, spiral range, nearest distance, number of FTS measurements during the overpass, and the column-integrated CO<sub>2</sub> abundances measured by in-situ instrumentations and FTS are given.

code	type	SZA [°] (min-max)	aircraft ceiling [km]	aircraft floor [m]	spiral [km] (ceiling,width)	nearest distance [km]	number of FTS data	FTS [ppm]	aircraft [ppm]
BIK_1	descent	56.2–61.1	11.5	500	(5,10)	0	65	378.3 ± 0.1	382.6 ± 0.1
BIK_2	ascent	56.2–61.1	8	500	(3,5)	0	67	378.3 ± 0.1	382.5 ± 0.2
BIK_3	descent	66.8–72.4	8	800	(5,8)	0	35	378.1 ± 0.2	382.5 ± 0.2
BIK_4	ascent	66.8–72.4	10.5	800	(5,10)	0	35	378.1 ± 0.2	382.5 ± 0.1
BRE_1	descent	58.0–75.5	13	500	(6,10)	0	30	379.1 ± 0.4	383.7 ± 0.1
BRE_2	descent	59.5–62.8	13	500	(10,10)	0	37	378.7 ± 0.4	383.5 ± 0.1
GAR_1	descent	53.9–62.3	12.5	1500	(7,15)	5	19	379.6 ± 0.3	384.1 ± 0.1
JEN_1	descent	59.0–63.8	12.5	800	(7,10)	0	8	379.7 ± 0.4	383.7 ± 0.1
JEN_2	ascent	59.0–63.8	8	800	–	0	8	379.7 ± 0.4	383.8 ± 0.2
JEN_3	descent	59.9–61.7	12.5	500	(9,15)	0	7	380.0 ± 0.3	384.1 ± 0.1
JEN_4	ascent	59.9–61.7	12.5	500	–	0	7	380.0 ± 0.3	384.1 ± 0.1
KAR_1		54.2–64.3	7	200	–	10	26	380.8 ± 0.3	384.6 ± 0.2
ORL_1	descent	68.9–83.6	11.5	700	(9,15)	30	45	380.1 ± 0.3	384.2 ± 0.1
ORL_2	ascent	68.9–83.6	7	700	(3,5)	0	45	380.0 ± 0.3	384.2 ± 0.2
ORL_3	descent	51.8–52.5	11	700	(8,30)	12	10	380.3 ± 0.4	384.1 ± 0.1
ORL_4	ascent	51.8–52.5	8	700	(5,5)	0	10	380.3 ± 0.4	384.2 ± 0.2

[Title Page](#)
[Abstract](#)
[Introduction](#)
[Conclusions](#)
[References](#)
[Tables](#)
[Figures](#)
[Back](#)
[Close](#)
[Full Screen / Esc](#)
[Printer-friendly Version](#)
[Interactive Discussion](#)


## The IMECC campaign: results for CO<sub>2</sub>

J. Messerschmidt et al.

**Table 6.** A linear relationship and a zero intercept are predicted. The scale factors are calculated by considering solely the IMECC campaign, by adding the IMECC campaign to the previous TCCON calibrations and in two worst ghosts scenarios (ghost\_O: all ghosts lead to CO<sub>2</sub> overestimation, ghost\_U: all ghosts lead to CO<sub>2</sub> underestimation). For comparison the scaling factor for the previous TCCON calibrations is listed as given in Wunch et al. (2010).

data	scale factor	uncertainty	
		best fit ( $\sigma$ )	scale factor ( $2\sigma$ )
IMECC calibration	0.989	0.001	0.002
IMECC (ghost_O)	0.991	0.001	0.002
IMECC (ghost_U)	0.988	0.001	0.002
IMECC and previous TCCON calibrations	0.989	0.001	0.002
previous TCCON calibrations	0.989	0.001	0.002

[Title Page](#)
[Abstract](#)
[Introduction](#)
[Conclusions](#)
[References](#)
[Tables](#)
[Figures](#)
[Back](#)
[Close](#)
[Full Screen / Esc](#)
[Printer-friendly Version](#)
[Interactive Discussion](#)


## The IMECC campaign: results for CO<sub>2</sub>

J. Messerschmidt et al.

Title Page

Abstract

Introduction

Conclusions

References

Tables

Figures

◀

▶

◀

▶

Back

Close

Full Screen / Esc

Printer-friendly Version

Interactive Discussion



**Table 7.** Results of the two retrieval approaches are listed. The differences are calculated by FTS retrieval (TCCON standard a priori) minus FTS retrieval (aircraft a priori).

	mean result (standard a priori)	mean result (aircraft a priori)	difference (1.col.–2.col.)
FTS $X_{\text{CO}_2}$	379.5	379.4	$0.0 \pm 0.1$
in-situ CO <sub>2</sub>	383.7	383.7	$0.0 \pm 0.1$

## The IMECC campaign: results for CO<sub>2</sub>

J. Messerschmidt et al.

Title Page

Abstract

Introduction

Conclusions

References

Tables

Figures

◀

▶

◀

▶

Back

Close

Full Screen / Esc

Printer-friendly Version

Interactive Discussion



**Table 8.** The scale factor calculated with (a) the use of the TCCON standard a priori, (b) the use of the TCCON standard a priori and including BRE\_1, JEN\_3 and JEN\_4 data, and (c) IMECC calibration as described in Sect. 4.1. All estimations are consistent within their uncertainties.

data	scale factor	uncertainty	
		best fit ( $\sigma$ )	scale factor ( $2\sigma$ )
TCCON standard retrieval	0.989	0.001	0.002
TCCON standard retrieval (KAR_1,BRE_1,JEN_3–4)	0.989	0.001	0.002
IMECC calibration	0.989	0.001	0.002

---

**The IMECC  
campaign: results for  
CO<sub>2</sub>**J. Messerschmidt et al.

---

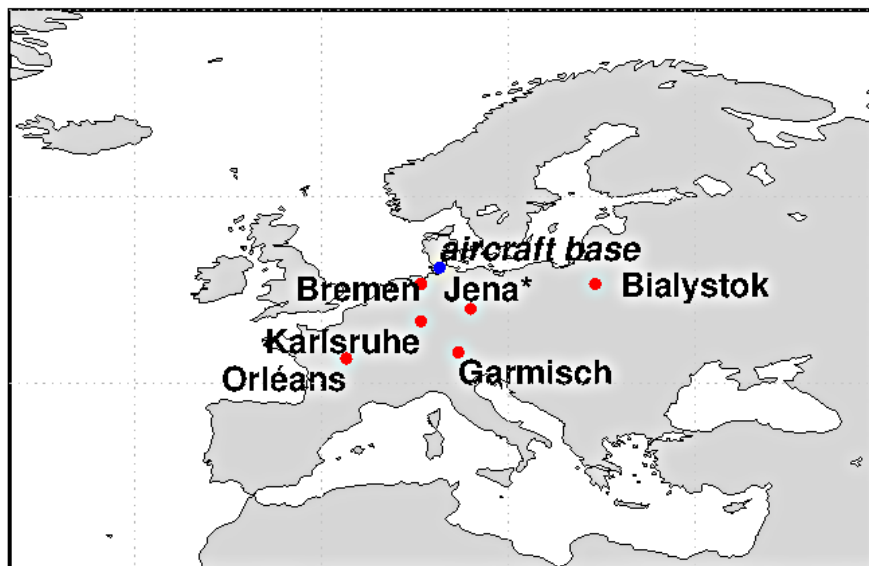


**Fig. 1.** A map of the five European TCCON sites, and a mobile FTS system located at Jena (indicated by Jena\*), which were calibrated with respect to WMO standards for the first time during the IMECC campaign.

[Title Page](#)[Abstract](#)[Introduction](#)[Conclusions](#)[References](#)[Tables](#)[Figures](#)[◀](#)[▶](#)[◀](#)[▶](#)[Back](#)[Close](#)[Full Screen / Esc](#)[Printer-friendly Version](#)[Interactive Discussion](#)

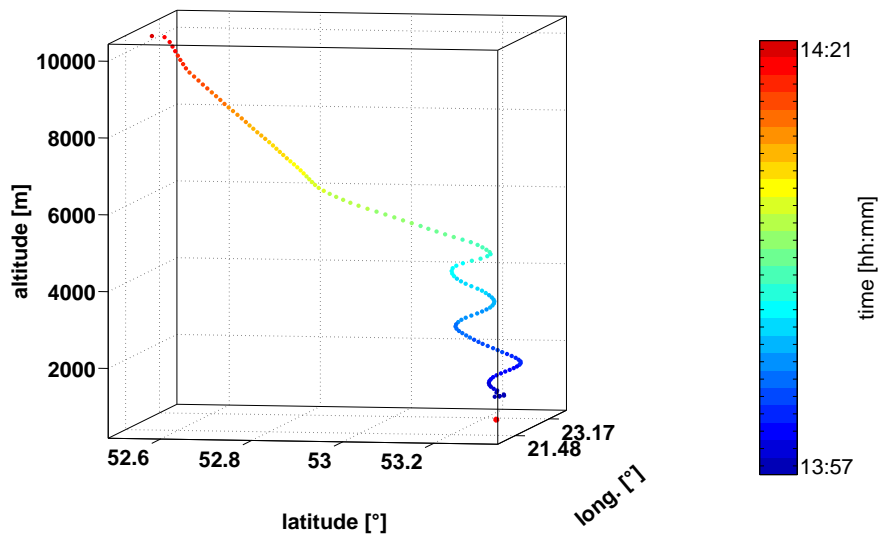


**Fig. 2.** BIK\_4: a typical aircraft profile as performed during the IMECC campaign. The participating European TCCON sites were approached typically at a flight altitude of 11 km. Close to the sites, a spiral was flown in the lower troposphere.

The IMECC campaign: results for CO<sub>2</sub>

J. Messerschmidt et al.

Title Page

Abstract Introduction

Conclusions References

Tables Figures

◀ ▶

◀ ▶

Back Close

Full Screen / Esc

Printer-friendly Version

Interactive Discussion



## The IMECC campaign: results for CO<sub>2</sub>

J. Messerschmidt et al.

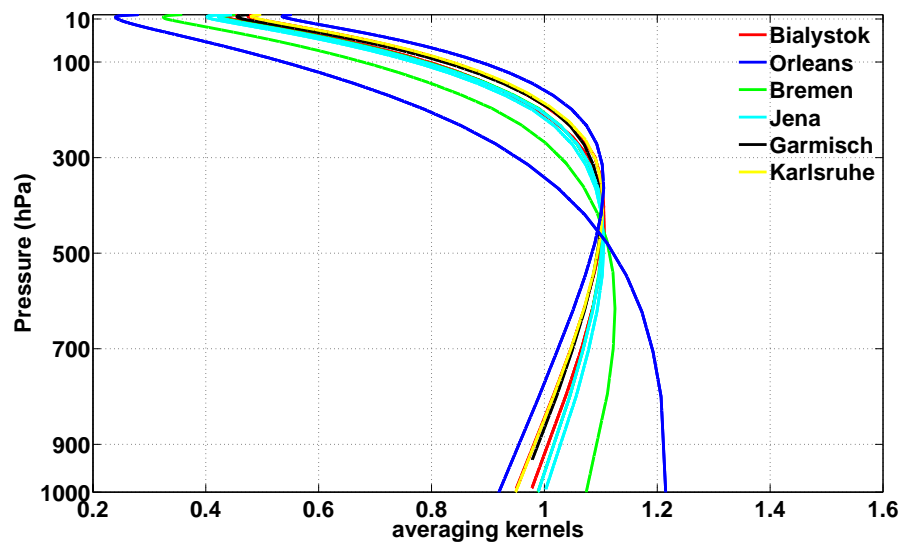


**Fig. 3.** All column averaging kernels for CO<sub>2</sub> used for the integration during the IMECC campaign. The colors indicate the associated site at which the FTS measurements were taken. Due to different solar zenith angles (SZAs), the averaging kernels vary for the various sites and overpass times. The SZAs are given in Table 5.

[Title Page](#)[Abstract](#)[Introduction](#)[Conclusions](#)[References](#)[Tables](#)[Figures](#)[◀](#)[▶](#)[◀](#)[▶](#)[Back](#)[Close](#)[Full Screen / Esc](#)[Printer-friendly Version](#)[Interactive Discussion](#)

## The IMECC campaign: results for CO<sub>2</sub>

J. Messerschmidt et al.

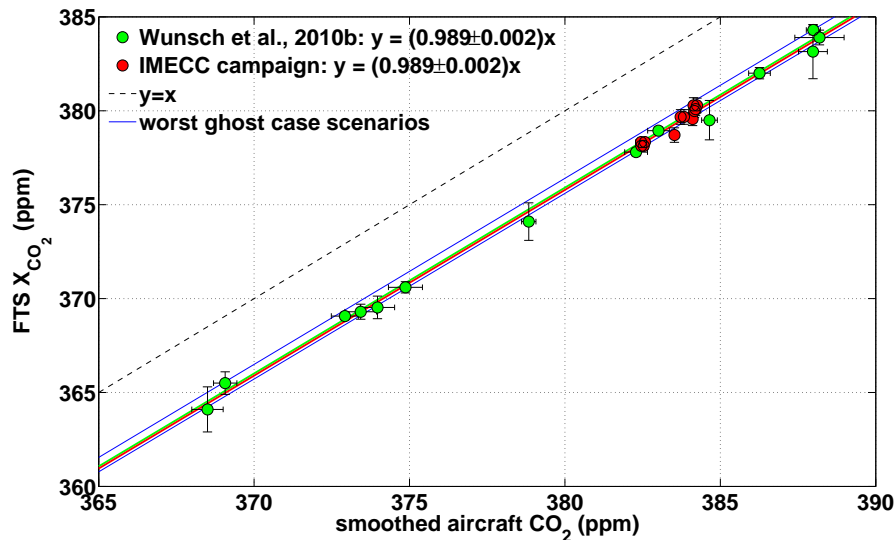


**Fig. 4.** The IMECC campaign in comparison with previous TCCON calibrations, published in Wunch et al. (2010). The scaling factors agree within their uncertainties. This suggests one global scaling factor can be used for CO<sub>2</sub> for all TCCON sites worldwide. With the thin blue lines the best fit to the worst ghost case scenarios are indicated.

Title Page

Abstract

Introduction

Conclusions

References

Tables

Figures

◀

▶

◀

▶

Back

Close

Full Screen / Esc

Printer-friendly Version

Interactive Discussion



## The IMECC campaign: results for CO<sub>2</sub>

J. Messerschmidt et al.

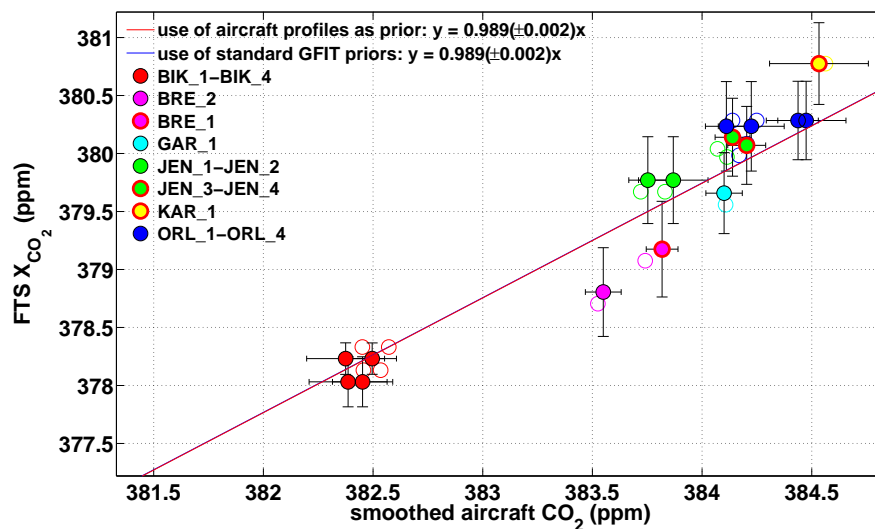


**Fig. 5.** The IMECC data were analyzed with the TCCON standard a priori profiles. The unconsidered KAR\_1, BRE\_1, JEN\_3, and JEN\_4 data are shown in the site corresponding color with red circles. The corresponding retrievals, with the aircraft profiles as a priori, are given as circles in the same color. The resulting scale factor is consistent (within the uncertainty) with the scale factors calculated using of the aircraft profiles as a priori (Sect. 4.1).

Title Page

Abstract

Introduction

Conclusions

References

Tables

Figures

◀

▶

◀

▶

Back

Close

Full Screen / Esc

Printer-friendly Version

Interactive Discussion



## The IMECC campaign: results for CO<sub>2</sub>

J. Messerschmidt et al.

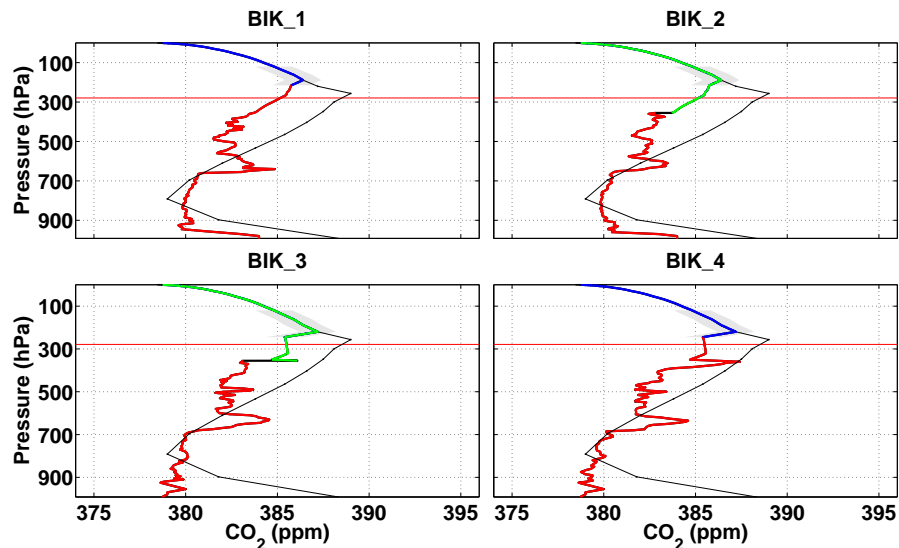


**Fig. A1.** The four assembled aircraft profiles taken in Bialystok. In BIK<sub>2</sub> and BIK<sub>3</sub> the aircraft had a flight height of 8 km, and the upper parts were replaced with the measurements of the contemporary overpasses BIK<sub>1</sub> and BIK<sub>4</sub>. The aircraft measurements are given in red. The GFIT a priori profile fitted in CO<sub>2</sub> to the aircraft measurements are shown in blue. Extended parts for missing measurements in the upper troposphere are indicated as black and used contemporary profiles in green. The NCEP tropopause height is indicated by a thin red line. The original GFIT a priori profiles are shown with a thin dotted black line.

[Title Page](#)[Abstract](#)[Introduction](#)[Conclusions](#)[References](#)[Tables](#)[Figures](#)[◀](#)[▶](#)[◀](#)[▶](#)[Back](#)[Close](#)[Full Screen / Esc](#)[Printer-friendly Version](#)[Interactive Discussion](#)

**The IMECC  
campaign: results for  
CO<sub>2</sub>**

J. Messerschmidt et al.

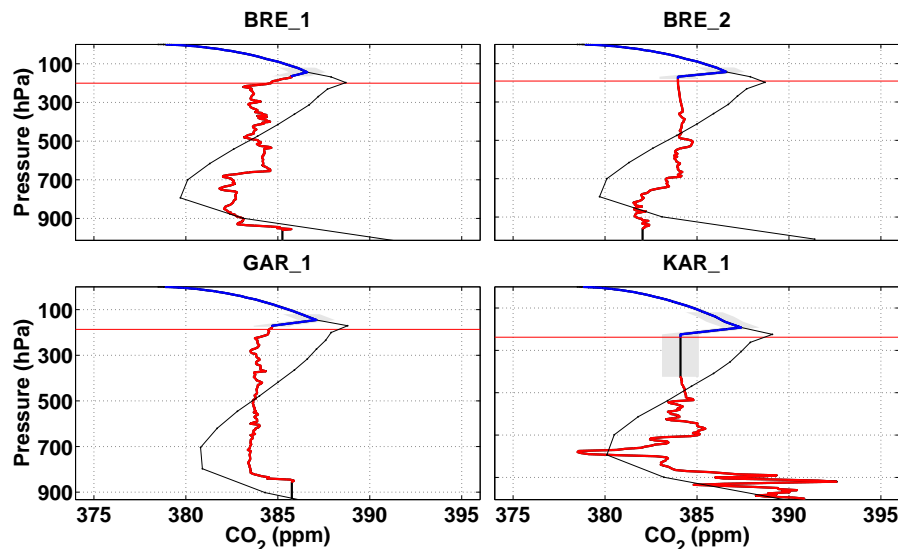


**Fig. A2.** In Bremen (BRE\_1, BRE\_2) and in Garmisch (GAR\_1), the aircraft ceiling reached the tropopause and the profiles could be completed by solely using the GFIT standard a priori. Due to bad weather conditions no aircraft profile was taken over the FTS site Karlsruhe. The presented in-situ data were collected while a stop-over 50 km south of the site. The Karlsruhe result was not considered in the IMECC calibration, but afterwards compared to the findings. Used color are explained in Fig. A1.

Title Page

Abstract

Introduction

Conclusions

References

Tables

Figures

◀

▶

◀

▶

Back

Close

Full Screen / Esc

Printer-friendly Version

Interactive Discussion



## The IMECC campaign: results for CO<sub>2</sub>

J. Messerschmidt et al.

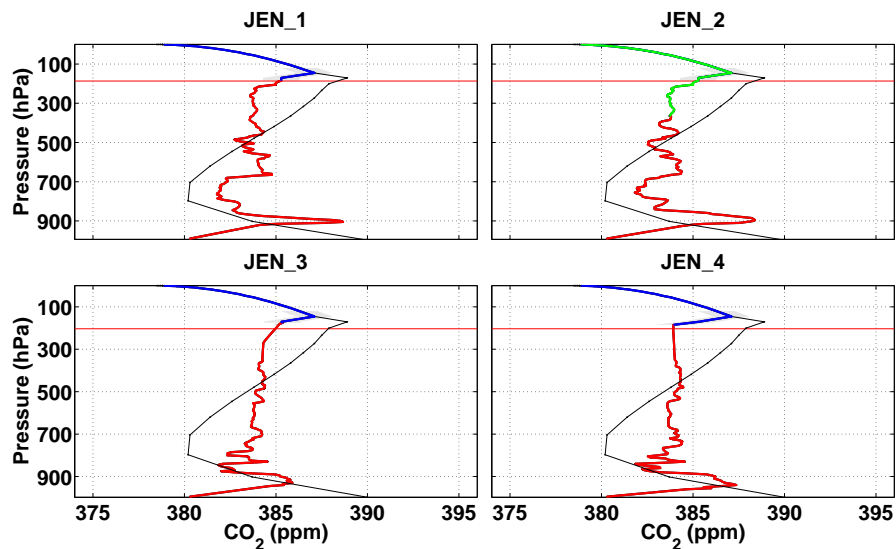


**Fig. A3.** Three out of four overpasses above the mobile FTS system in Jena reached the tropopause. The JEN\_2 profile was extended by replacing the upper part with the aircraft profile of JEN\_1. The color indication is the same as in Fig. A1.

[Title Page](#)[Abstract](#)[Introduction](#)[Conclusions](#)[References](#)[Tables](#)[Figures](#)[◀](#)[▶](#)[◀](#)[▶](#)[Back](#)[Close](#)[Full Screen / Esc](#)[Printer-friendly Version](#)[Interactive Discussion](#)

## The IMECC campaign: results for CO<sub>2</sub>

J. Messerschmidt et al.

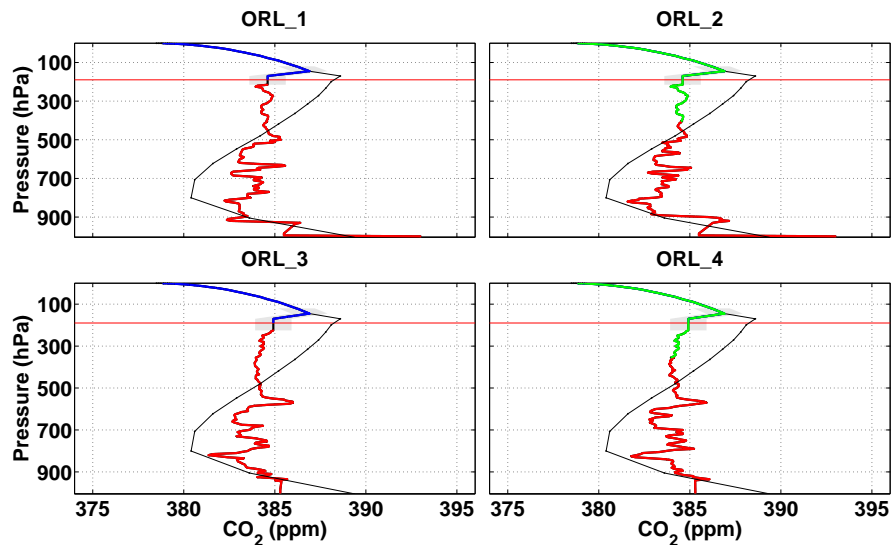


**Fig. A4.** Two out of four aircraft profiles could be measured up to the tropopause at the European TCCONsite in Orléans. The upper tropospheric portions in ORL\_2 and ORL\_4 are substituted by the measurements of ORL\_1 and ORL\_3. All aircraft profiles were taken at one day, two at low solar angle and two at higher solar angle around noon. Color description is given in Fig. A1.

[Title Page](#)[Abstract](#)[Introduction](#)[Conclusions](#)[References](#)[Tables](#)[Figures](#)[◀](#)[▶](#)[◀](#)[▶](#)[Back](#)[Close](#)[Full Screen / Esc](#)[Printer-friendly Version](#)[Interactive Discussion](#)